Materials Chemistry and Physics 123 (2010) 557–562

Contents lists available at ScienceDirect

Materials Chemistry and Physics

journal homepage: www.elsevier.com/locate/matchemphys

Cobalt and KNO_3 supported on alumina catalysts for diesel soot combustion

Claudia B. Grzona[a], Ileana D. Lick[b], Enrique Rodriguez Castellón[c], Marta I. Ponzi[a], Esther N. Ponzi[b,*]

[a] 25 de mayo 284, INTEQUI-CONICET-UNSL, Facultad de Ingeniería y Ciencias Económico-Sociales, Villa Mercedes, 5730, Argentina
[b] Calle 47 N° 257, CINDECA (CCT-LaPlata-CONICET-UNLP), Departamento de Química, Facultad de Ciencias Exactas, La Plata, 1900, Argentina
[c] Departamento de Química Inorgánica, Cristalografía y Mineralogía, Facultad de Ciencias, Universidad de Málaga, Campus de Teatinos, Málaga, 29071, Spain

ARTICLE INFO

Article history:
Received 21 April 2009
Received in revised form 1 October 2009
Accepted 7 May 2010

Keywords:
Diesel soot
Combustion
KNO_3
Cobalt

ABSTRACT

The catalytic combustion of diesel soot was studied in the presence of fresh and aged catalysts: Co/Al_2O_3, KNO_3/Al_2O_3 and $Co/KNO_3/Al_2O_3$. The catalysts were prepared by impregnation using nitrate solutions. The catalysts were characterized by X-ray diffraction, thermal programmed reduction, vibrational spectroscopy and X-ray photoelectron spectroscopy.

Fresh and aged catalysts present high activity in presence of O_2 and O_2/NO. The values of the combustion temperature decrease more than 200 °C with respect to that observed in the process without catalysis. The activity is associated with the presence of KNO_3 and the role of this salt can be attributed to the contribution of NO_3^-/NO_2^- redox cycle.

1. Introduction

Emissions of diesel engines contain among other contaminants, carbon oxides, nitrogen oxides, hydrocarbons and particulate matter in their composition. In order to preserve the environment, it is necessary to regulate emissions and to stimulate the search of new technologies able to decrease concentration of contaminants.

In the particular case of particulate matter, mainly composed by soot, it is possible to place a filter in the automobile exhaust pipe where the material is retained and removed by oxidation, thus avoiding the material accumulation with the consequent increase of pressure fall and decrease of engine efficiency.

The non-catalytic combustion of particulate matter occurs at higher temperatures than the temperature of effluent gases. To decrease the oxidation temperature of particulate matter, oxidation catalysts are used since they are able to burn the soot without need of an additional heat source. Among oxidation catalysts reported as active there are those ones that contain alkali metals in their composition [1–16].

Studies previously performed show that potassium nitrate supported on simple oxides presents a good catalytic activity and that the incorporation of copper in the catalyst formula improves the selectivity of carbon combustion to carbon dioxide [17,18]. The role of KNO_3 can be associated to: (i) increase of contact between soot and surface of the catalyst with the increase of possible effective collisions between soot and catalyst, generated by the melting of potassium nitrate on the catalytic surface, (ii) a redox reaction in which the nitrate is reduced to nitrite by reaction with carbon and again reoxidized to nitrate [18–21]. Water vapor can also affect to the performance of the catalysts since deactivation can occur due to chemical modifications that are more pronounced at high temperatures.

The aim of this work is the study of fresh and aged catalysis for the diesel soot oxidation reaction in the presence of O_2/inert and NO/O_2/inert. Furthermore, several characterization techniques have been performed to study the nature of cobalt and potassium and potassium nitrate.

2. Experimental

2.1. Preparation of catalysts

Precursors of catalysts containing cobalt and/or potassium nitrate were prepared by impregnation of gamma-alumina with an aqueous solution of $Co(NO_3)_2$ and/or KNO_3 in a rotavapor equipment. The equipment operates at 160 rpm, bath temperature 50 °C and vacuum pressure 50 mm Hg. The precursors were dried at 80 °C for 24 h and were named PCo/Al_2O_3, $PKNO_3/Al_2O_3$ and $PCo/KNO_3/Al_2O_3$.

Catalysts with a nominal cobalt content of 5% and/or a potassium nitrate content of 25% (%w/w K = 9.6 and %w/w NO_3^- = 15.4) were prepared by calcination of precursors at 600 °C for 2 h. Catalysts were generically denoted as Co/Al_2O_3, KNO_3/Al_2O_3 and $Co/KNO_3/Al_2O_3$.

2.2. Aging experiments with feed containing water vapor

Aging experiments were carried out on samples of fresh catalyst loaded in a quartz reactor fed with a gaseous current (QTotal = 30 ml min^{-1}) containing 10% O_2 and 90% N_2 saturated with water vapor (7 vol%). Aging treatments were performed at 800 °C for 2 h.

* Corresponding author. Tel.: +54 221 4211353.
E-mail address: eponzi@quimica.unlp.edu.ar (E.N. Ponzi).

0254-0584/$ – see front matter © 2010 Elsevier B.V. All rights reserved.
doi:10.1016/j.matchemphys.2010.05.014

Table 1
Chemical analysis according to AAS and size of Co_3O_4 crystals in fresh and aged catalysts.

Catalyst	Co[a] (wt%)	K[a] (wt%)	NO_3^- exp.[b] (wt%)	NO_3 estimated[c] (wt%)
KNO_3/Al_2O_3 fresh	–	9.50	7.91	15.10
KNO_3/Al_2O_3 aged	–	7.50	0.11	11.9
$Co/KNO_3/Al_2O_3$ fresh	4.85	9.00	10.45	14.3
$Co/KNO_3/Al_2O_3$ aged	4.85	8.00	0.42	12.7
Co/Al_2O_3 fresh	4.95	–		
Co/Al_2O_3 aged	4.95	–		

[a] By AAS.
[b] By UV–vis spectroscopic method.
[c] Calculated from %w/w K content.

2.3. Characterization of catalysts

Cobalt and potassium contents were determined by atomic absorption spectrophotometry with a spectrophotometer PerkinElmer AA 800.

The content of soluble nitrate ions in the catalyst was determined by UV–vis spectroscopic measurements at ~224 nm where the absorption spectrum for nitrate (NO_3^-) has a peak that is proportional to the nitrate concentration.

Crystalline phases within the catalysts were identified by powder X-ray diffraction (XRD) analysis using a Rigaku D-Max III diffractometer equipped with Ni-filtered Cu Kα radiation at $1^\circ\,min^{-1}$. The crystal size was calculated using the Scherrer equation and was determined with a scanning rate of $1/8^\circ\,min^{-1}$.

TPR (temperature programmed reduction) experiments were carried out with the conventional equipment. The TPR was performed using 10% hydrogen in nitrogen (flow rate = 20 $cm^3\,min^{-1}$) with a heating rate of 10 °C min^{-1} up to 950 °C. The sample loaded was 20 mg.

The presence of nitrate anions on precursors and catalysts was studied by means of FTIR spectroscopy using a Bruker EXINOX 55 equipment. Spectra were recorded at ambient temperature in the 4000–400 cm^{-1} range and the samples were prepared in form of pills with KBr.

The X-ray photoelectron spectroscopy (XPS) was performed with a spectrometer Physical Electronics PHI-5700, equipped with a dual X-ray source of Mg Kα (1253.6 eV) and Al Kα (1486.6 eV) and a multi-channel detector. Spectra of powdered samples were recorded in the constant pass energy mode at 29.35 eV, using a 720 μm diameter analysis area. Charge referencing was measured against adventitious carbon (C 1s at 284.8 eV). A PHI ACCESS ESCA-V6.0 F software package was used for acquisition and data analysis. A Shirley-type background was subtracted from the signals. Recorded spectra were always fitted using Gaussian–Lorentzian curves in order to determine the binding energy of the different element core levels more accurately.

2.4. Catalytic measurements

The soot sample used in this work is synthetic flame soot named Printex-U manufactured by Degussa. This carbon is commonly used to substitute diesel soot in academic studies. Thermal programmed oxidation techniques were used to carry out the catalytic tests. In these techniques the contact between the catalyst and the soot is an important factor. When this contact is poor (loose contact) the catalysts can be less active than when the contact is tight. The first type of contact is more representative for practical applications.

In this work two equipments were used to carry out catalytic experiments: a thermogravimetric reactor with an O_2/He feed and a fixed bed reactor with NO/O_2/He or O_2/He feed. In the first case, the soot combustion was performed in a thermobalance (TGA-50 Shimadzu) with a heating rate of 10 °C min^{-1} and an O_2/He feed (2:1). In order to carry out activity experiments, the soot and the catalyst, in a 1/10 ratio, were milled carefully in an agate mortar before introduction into the reactor (tight contact). The weight loss and the temperature were recorded as a function of time. The derivative curve (DTG) was obtained from the weight loss information as a function of time, and from this curve the temperature where the combustion rate is maximum (T_{max}). In the second case, a quartz reactor (i.d. = 0.8 cm) was used simulating conditions near to the ones found in an exhaust pipe (loose contact, NO presence, high space velocity and 8% of O_2). The mixture composition was 8 vol% of O_2 and 1500 ppm of NO (total flow = 50 ml min^{-1}). The mass of soot/catalyst (1/10, w/w) loaded in the reactor was 33 mg. The soot was mixed with the catalyst with spatula (loose contact). The temperature range studied between 200 °C and 700 °C and the heating rate 2 °C min^{-1}. Reaction products were analyzed with a gas chromatograph Shimadzu model GC-8A provided with a TCD detector. The separation of products was carried out in a concentric column CTRI of Altech. This system permitted identification and quantification of O_2, CO_2 and CO peaks. The amount of combusted soot was calculated from the chromatographic information of CO_2 and CO.

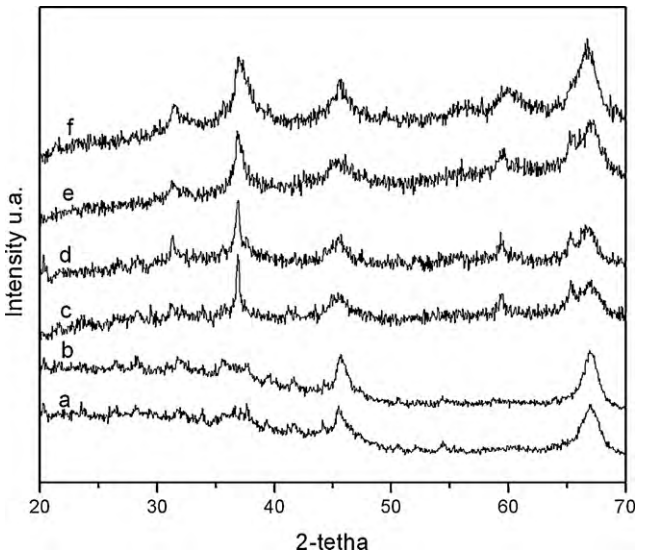

Fig. 1. XRD diagrams of fresh and aged catalysts: (a) fresh KNO_3/Al_2O_3, (b) aged KNO_3/Al_2O_3, (c) fresh $Co/KNO_3/Al_2O_3$, (d) aged $Co/KNO_3/Al_2O_3$, (e) fresh Co/Al_2O_3, and (f) aged Co/Al_2O_3.

3. Results

3.1. Chemical analysis

Cobalt and potassium contents in fresh and aged catalysts were obtained by means of atomic absorption spectroscopy and it is shown in Table 1. In the same table, the content of soluble nitrate ions is shown obtained by the UV–vis spectroscopic method.

Results obtained indicate that the cobalt concentration of Co/Al_2O_3 and $Co/KNO_3/Al_2O_3$ catalysts is very near to the nominal one and that the aging treatment does not modify the concentration of this transition metal.

The potassium concentration in fresh catalysts is near to the nominal value (9.6%, w/w) and the aging treatment decreases such concentration. The aged $Co/KNO_3/Al_2O_3$ catalyst loses 11% potassium and the KNO_3/Al_2O_3 catalyst loses 21% with respect to the fresh catalyst concentration.

Table 1 also includes the soluble nitrate content determined by UV–vis spectroscopy in the washing water. Fresh catalysts contain soluble nitrate in their composition and the content is noticeably lower than the nominal value (15.4%, w/w). This would indicate that during precursor calcination, a nitrate part is decomposed. The $Co/KNO_3/Al_2O_3$ catalyst shows higher content of soluble nitrate ions than in the case of the KNO_3/Al_2O_3 catalyst. The aging treatment decreases substantially the content of soluble nitrate ions.

Since the aging at 800 °C for 2 h partially modifies the potassium content and even more noticeably the soluble nitrate content, it is possible to postulate that the nitrate interacts with the catalyst being transformed into a nitrate coordinate with the support (insoluble) or that the potassium nitrate decompose to K_2O. Also, part of the KNO_3 can be lost by volatilization due to the high temperature (800 °C) of the ageing treatment.

3.2. X-ray diffraction (XRD)

XRD measurements were carried out to analyze the presence of crystalline species in fresh and aged catalysts. Fig. 1 shows the corresponding diagrams.

The XRD diagram of fresh Co/Al_2O_3 catalyst shows typical signals of the Co_3O_4 spinel whose more intense lines are found at 2-theta = 36.8°, 65.35°, 31.2° and 59.35°. The aged Co/Al_2O_3 catalyst presents a similar diagram. Taking into account that the catalyst was aged for 2 h at 800 °C, the incipient formation of the cobalt aluminate spinel, $CoAl_2O_4$, could be expected whose XRD lines coincide with the lines of the Co_3O_4 spinel.

In the XRD diagrams of the fresh and aged $Co/KNO_3/Al_2O_3$ catalyst, XRD lines associated with the presence of cobalt oxidic species, Co_3O_4, are observed. In these diagrams, neither XRD lines associated to crystalline species of KNO_3 (2-theta = 24.7° and 31°) nor of K_2O (2-theta = 37.7°, 30.6°, 32.3°, 31.23°, and 49.79°) are observed.

In the XRD diagrams of fresh and aged KNO_3/Al_2O_3 catalyst, neither KNO_3 nor K_2O signals are observed.

The Co_3O_4 crystallinity in fresh as well in aged catalysts is higher in catalysts containing potassium nitrate.

The aging at high temperature in the presence of water vapor generates a decrease in the crystallinity of Co_3O_4 spinel in catalysts. The lower crystallinity can be attributed also to an amorphisation of the surface leading to a decrease of the longer distances in the cluster. This fact can be due to the diffusion of cobalt ions into the spinel framework with alumina vacancies. Such process has been previously observed in the case of Co/SiO_2 [22].

3.3. Temperature programmed reduction (TPR)

Fig. 2 shows temperature programmed reduction diagrams TPR of fresh catalysts and Co_3O_4 bulk.

The Co_3O_4 spinel reduces between 300 and 500 °C with reduction of Co^{+3} to Co^{2+} and subsequent reduction of Co^{2+} to Co^0 [23]. The TPR diagram of fresh Co/Al_2O_3 catalyst shows a very broad band where the reduction occurs between 380 °C and 800 °C. The first reduction zone of catalyst is attributed to the segregated Co_3O_4 spinel reduction and reduction signals above 600 °C are attributed to cobalt(II) species reduction interacted with the support. The gamma-alumina presents a defect spinel structure with vacant cation sites, this structure allows the diffusion of cobalt ions into the oxidic matrix to generate incomplete spinels (non-stoichiometric cobalt aluminate) [24].

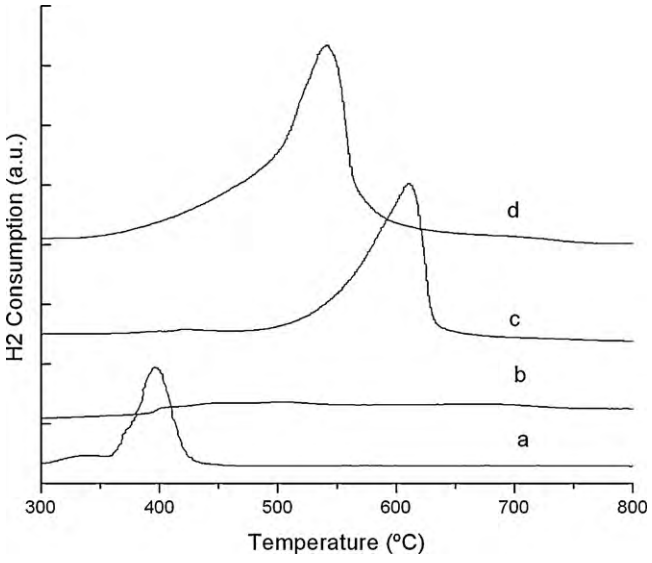

Fig. 2. Temperature programmed reduction diagrams: (a) Co_3O_4, (b) fresh Co/Al_2O_3, (c) fresh KNO_3/Al_2O_3, and (d) fresh $Co/KNO_3/Al_2O_3$.

Table 2
Gibbs free energy change in reduction reactions with hydrogen.

Temperature (°C)	ΔG (kJ)			
	Reaction (1)	Reaction (2)	Reaction (3)	Reaction (4)
0	−134.184	−31.642	−704.527	21.285
100	−142.090	−73.842	−715.076	17.726
200	−148.872	−112.543	−720.511	14.689
300	−154.676	−148.684	−722.271	12.026
400	−158.770	−181.321	−719.712	9.594
500	−163.190	−211.898	−714.482	7.277
600	−168.099	−241.301	−707.615	5.081
700	−172.672	−269.713	−699.402	2.980
800	−176.953	−298.879	−691.674	0.934
900	−180.978	−328.374	−684.067	−1.087

The TPR diagram of KNO_3/Al_2O_3 catalyst presents an important reduction signal between 500 °C and 650 °C, with a maximum at 615 °C, assigned to the potassium nitrate reduction [18,20]. The potassium nitrate can be reduced with H_2 generating KNO_2, NO and NH_3.

$$KNO_3 + H_2(g) = KNO_2 + H_2O(g) \quad (1)$$

$$2KNO_3 + 3H_2(g) = 2NO(g) + K_2O + 3H_2O(g) \quad (2)$$

$$2KNO_3 + 8H_2(g) = 2NH_3(g) + K_2O + 5H_2O(g) \quad (3)$$

Table 2 shows estimations of Gibbs free energy change noticing that the proposed reactions can occur.

The TPR diagram of $Co/KNO_3/Al_2O_3$ catalyst presents a reduction signal starting from 350 °C, with a maximum at 545 °C. This signal involves the reduction of cobalt and nitrate species. The cobalt presence increases the nitrate reducibility probably by hydrogen activation originated in the metallic cobalt decreasing the peak temperature (approx. 70 °C). The reduction of Co will promote the reduction of nitrates by hydrogen spillover, because hydrogen can be dissociated on the reduced Co; such hydrogen spills to the nitrate ions and reduces them [25–27].

TPR diagrams of aged catalysts show reduction signals of very low intensity. The lowest reduction of aged Co/Al_2O_3 catalyst is attributed to cobalt aluminate incipient formation which is not thermodynamically reducible (reaction (4)) below 800 °C as it is shown in results of Table 2.

$$CoAl_2O_4 + H_2(g) = Co + H_2O + Al_2O_3 \quad (4)$$

Table 3 shows the areas of the TPR peaks of fresh and aged catalysts. The areas of the peaks of aged catalysts containing potassium nitrate are substantially lower than that observed in the case of fresh catalysts, evidencing a nitrate species partial loss.

Table 3
Quantitative TPR results: mmol consumed H_2 obtained with fresh and aged catalysts.

	H_2 consumption (mmol H_2)	H_2 consumption for the nitrate ion reduction
Co/Al_2O_3	0.041	–
KNO_3/Al_2O_3	0.082	0.082
$Co/KNO_3/Al_2O_3$	0.130	0.089[a]
Co/Al_2O_3 aged	0.010	–
KNO_3/Al_2O_3 aged	0.005	0.005
$Co/KNO_3/Al_2O_3$ aged	0.027	0.017[a]

[a] Estimated as the difference between the total value and the one corresponding to cobalt of catalyst without potassium nitrate.

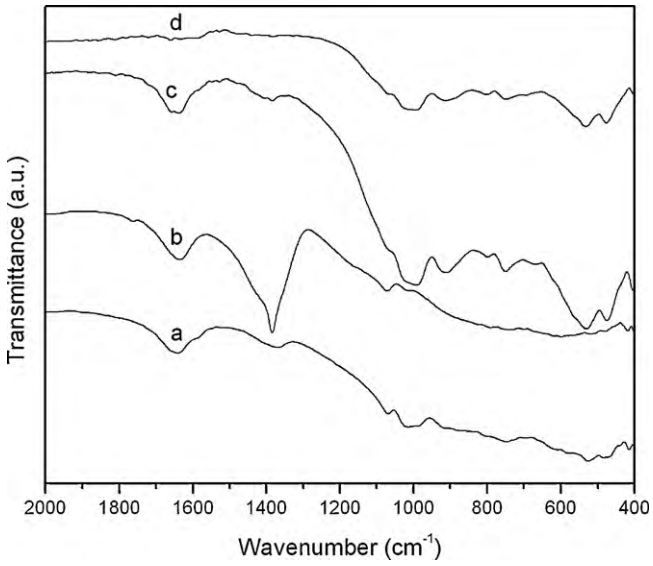

Fig. 3. FTIR spectra of support, precursor and cobalt catalysts: (a) alumina, (b) PCo/Al_2O_3 (precursor), (c) fresh Co/Al_2O_3, and (d) aged Co/Al_2O_3.

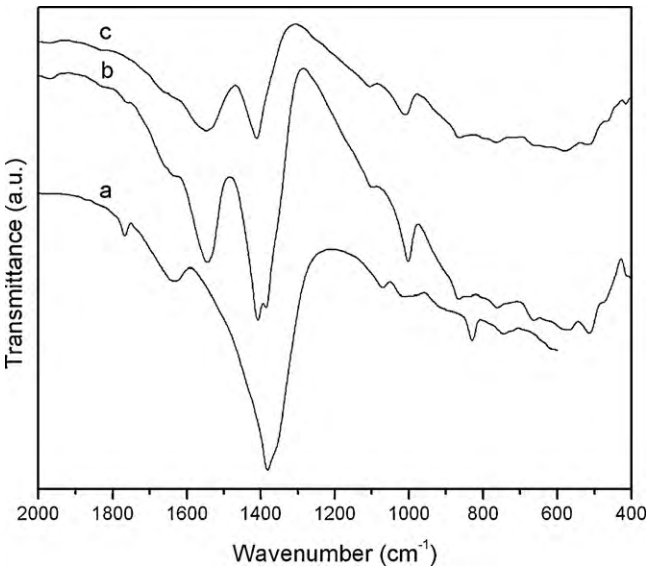

Fig. 5. FTIR spectrum of precursor and Co/KNO_3 catalysts: (a) $PCo/KNO_3/Al_2O_3$ (precursor), (b) fresh $Co/KNO_3/Al_2O_3$, and (c) aged $Co/KNO_3/Al_2O_3$.

3.4. Vibrational spectroscopy by FTIR

Fig. 3 shows FTIR spectra of the following samples: precursor of cobalt catalyst and of fresh and aged Co/Al_2O_3 catalyst as well as of the support (gamma-alumina). In the precursor spectrum, it is possible to observe a band associated to the N–O antisymmetric stretching of nitrate ions (1385 cm^{-1}) coming from cobalt nitrate [28]. Spectra of fresh and aged Co/Al_2O_3 catalyst show signals in the zone 500–700 cm^{-1} that can be associated with the presence of cobalt species (Co_3O_4 or $CoAl_2O_4$).

Fig. 4 shows FTIR spectra of the following samples: potassium nitrate, catalyst precursor and fresh and aged KNO_3/Al_2O_3 catalyst. The potassium nitrate presents the band of the antisymmetric stretching mode typical of free nitrate ions (1385 cm^{-1}) and the band associated to the angular antisymmetric deformation O–N–O placed at 830 cm^{-1}. These signals are observed in the catalyst precursor spectrum. The spectrum of fresh KNO_3/alumina catalyst presents the signal at 1385 cm^{-1} evidencing the presence of free nitrate ions and besides it shows bands placed at 1410 cm^{-1} and 1540 cm^{-1} associated to the presence of monodentate and bidentate nitrate species. The aged catalyst spectrum shows a weak band associated to the presence of free nitrate ions and besides it presents two shoulders at 1420 cm^{-1} and 1540 cm^{-1} evidencing the presence of coordinated nitrate groups [28,29].

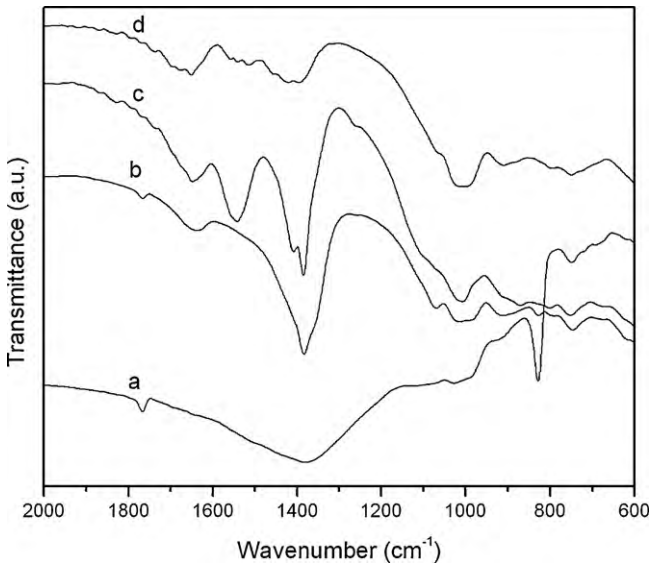

Fig. 4. FTIR spectra of KNO_3, precursor and KNO_3 catalysts: (a) KNO_3, (b) $PKNO_3/Al_2O_3$ (precursor), (c) fresh KNO_3/Al_2O_3, and (d) aged KNO_3/Al_2O_3.

Also, it is possible to observe in fresh and aged catalyst spectra, the energy absorption band placed at 1070–1010 cm^{-1} assigned to the N–O symmetric stretching mode, which is inactive when the nitrate ion is completely free.

Fig. 5 shows FTIR spectra of precursor and fresh and aged $Co-KNO_3/Al_2O_3$ catalysts. The precursor spectrum contains bands of potassium nitrate salt. Spectra of fresh and aged catalyst show characteristic bands of nitrate ions, and the fresh catalyst presents a band widening corresponding to the antisymmetric stretching mode of free nitrates and an unfolding of such band with higher signal intensity toward higher wavenumber (1410 cm^{-1}) characteristic of monodentate coordinated nitrates. Besides, it presents an intense band at 1545 cm^{-1} assigned to nitrate species coordinated as bidentate. In the case of the aged catalyst spectrum, the mentioned signals are of lower intensity and the signal at 1385 cm^{-1} is not observed.

These results indicate that the aging at high temperature produces modifications in the nature of potassium nitrate species, which reach higher interaction with the support.

3.5. X-ray photoelectron spectroscopy (XPS)

The XPS technique was performed to study the nature of cobalt and potassium as well as the chemical composition at superficial level.

The cobalt spectrum in an oxidic environment is a complex spectrum due to the possibility of the existence of more than one oxidation state (Co^{2+} and/or Co^{3+}) and different coordinations. Cobalt species proposed by the other characterization techniques tested are Co_3O_4 and Co^{2+} ions forming part of the cobalt aluminate incomplete spinel. The Co_3O_4 oxide contains Co(III) ions in octahedral coordination with an electronic configuration $t2g^6$ and $S = 0$ and Co(II) ions in tetrahedral coordination with electronic configuration eg^4teg^3 and $S = 3/2$, maintaining a ratio Co(II)/Co(III) = 1/2. The incomplete cobalt aluminate has Co(II) ions in tetrahedral coordination.

Table 4
XPS results for catalysts (all values in eV).

Co 2	Co $2p_{3/2}$	Co $2p_{3/2\ sat}$	pp-sat[a]	Co $2p_{1/2}$	Co $2p_{1/2\ sat}$	ΔE[b]	K $2p_{3/2}$	K $2p_{1/2}$
Co/Al_2O_3	779.7–781.6	786.3	6.6	795.7	803.25	16.0	–	–
$Co/KNO_3/Al_2O_3$	779.7	785.7	6.0	794.7	803.74	15.0	292.9	295.6
KNO_3/Al_2O_3		–	–	–	–	–	292.9	295.6

[a] Difference between main peak and satellite in eV.
[b] Difference between main Co $p_{3/2}$ and Co $p_{1/2}$ peaks in eV.

The core level cobalt spectrum shows de doublet Co $2p_{3/2}$ and Co $2p_{1/2}$ at about 781 eV and 795 eV, respectively with their respective shake-up satellites. The existence of satellite bands is associated with the presence of paramagnetic species and for this reason this signal is associated with the presence of Co(II) ($S = 3/2$) ions. In order to elucidate the nature of cobalt species, binding energies of Co $2p_{3/2}$ peak components can be observed. The Co_3O_4 presents core level Co $2p_{3/2}$ signals at 779.6 eV of Co(III) and at 780.7 eV of Co(II). The cobalt aluminate bulk presents a signal at 781.5 eV of Co(II) [30–32]. Table 4 shows the binding energies of peaks found in the core level Co 2p spectrum of catalysts Co/Al_2O_3 and $Co/KNO_3/Al_2O_3$. However, before performing the analysis of results it is necessary to mention that the cobalt spectrum intensity in the Co/Al_2O_3 catalyst is higher than the cobalt spectrum intensity in the $Co/KNO_3/Al_2O_3$ catalyst. The component of lower energy (at about 780 eV) associated to the Co_3O_4 presence can be observed in both spectra. The 782 eV component associated to the presence of Co(II) ions was only observed in the spectrum of Co/Al_2O_3 catalyst, however, as both spectra have the satellite peak (shake-up), the existence of Co(II) species is evident. These Co(II) ions can come from the Co_3O_4 or from Co(II) ions directly interacted with the oxidic matrix. According to bibliography, in the Co_3O_4 spectrum, the energy difference between the principal peak (pp) and its shake-up satellite (sat) is 10 eV and in the aluminate, the energy difference is 5 eV [33]. This difference is lower than 10 eV in samples tested, for this reason it is possible to propose the presence of Co(II) ions with interaction with the support. Besides, the potassium presence does not generate an appreciable change in the binding energy of cobalt at superficial level.

The core level K 2p spectrum presents a doublet K 2p level located at about 293 eV (K $2p_{3/2}$) and 296 eV (K $2p_{1/2}$) [8]. This binding energy found corresponds with the binding energy of potassium in the KNO_3. Also, the obtained results indicate that the cobalt presence does not modify the potassium binding energy.

Table 5 shows superficial Co, K, Al and O atomic concentrations of the three catalysts.

Concerning to cobalt, the obtained chemical composition indicate that the cobalt is found more exposed in the Co/Al_2O_3 catalyst than in the $Co/KNO_3/Al_2O_3$ catalyst. On the other hand, potassium is found more exposed in the $Co/KNO_3/Al_2O_3$ catalyst than in the KNO_3/Al_2O_3 catalyst. These results indicate that potassium nitrate remains at superficial level covering the catalytic surface.

3.6. Catalytic results obtained in a thermogravimetric reactor

These experiments were carried out in air/He flow with heating rate 10 °C min^{-1}. Values of initial combustion temperature (T_{ini}) and the temperature of maximum combustion rate (T_{max}) as well as the activation energy and the pre-exponential (A) expressed in 1/seg are summarized in Table 6. Kinetics calculations are made assuming the behavior of differential reactor and a kinetic expression of first order with respect to the soot (C) [18].

Table 5
Surface chemical composition in atomic concentration %.

Sample	Co	K	Al	O
Co/Al_2O_3	2.3	–	33.3	64.3
KNO_3/Al_2O_3	–	10.1	23.8	66.1
$Co/KNO_3/Al_2O_3$	0.2	15.9	15.3	68.5

Table 6
Results of TPO experiments performed in a thermogravimetric reactor.

Catalyst	T_{ini} (°C)	T_{max} (°C)	E_a (kJ mol^{-1})	ln(A)
Soot	520	640	171	18
Co/Al_2O_3	505	580	188	21
Co/Al_2O_3 aged	496	598	266	31
KNO_3/Al_2O_3	310	394	137	20
KNO_3/Al_2O_3 aged	362	410	118	16
$Co/KNO_3/Al_2O_3$	364	418	108	13
$Co/KNO_3/Al_2O_3$ aged	383	420	104	13

The temperature at which the combustion rate is maximum (T_{max}) for combustion without catalyst is around 640 °C, this temperature noticeably decreases when oxidation catalysts are used. The cobalt catalyst supported on alumina presents the maximum burning rate at 580 °C. Catalysts containing potassium nitrate in its composition KNO_3/Al_2O_3 and Co-KNO_3/Al_2O_3 present the maximum burning rate at 394 °C and 418 °C, respectively, and with low activation energy values (137 and 108 kJ mol^{-1}).

The results obtained when using aged catalysts in water vapor presence indicate that the catalysts maintain their activity. Initial temperatures obtained with catalysts containing potassium nitrate are lower than 385 °C, which is within the operation range of an exhaust pipe and the activation energy does not suffer significant modifications.

3.7. Catalytic results obtained in a reactor of fixed bed fed with NO/O_2

Fig. 6 shows catalytic results obtained in a reactor of fixed bed fed with a NO/O_2 mixture. In combustion experiments, 3 mg of particulate matter and 30 mg catalyst were used and mixed with spatula ("loose contact"). Curves represent the combustion evolution of particulate matter as function of the temperature in presence of fresh and aged catalysts.

The curve corresponding to the combustion reaction of particulate matter in catalyst absence shows that the temperature of the maximum is 585 °C.

The fresh Co/Al_2O_3 catalyst shows the maximum particulate matter conversion at 495 °C. Catalysts containing in their composition potassium nitrate, KNO_3/Al_2O_3 and $Co/KNO_3/Al_2O_3$, present lower combustions temperatures at 372 °C and 384 °C, respectively.

The aging treatment for 2 h at 800 °C does not generate activity loss for these catalysts.

3.8. Catalytic activity and active species

The reaction mechanism proposed for catalysts containing potassium nitrate is the soot oxidation with a concomitant reduction of nitrate ion to nitrite (step 1) completing the catalytic cycle with nitrite oxidation by gaseous oxygen (step 2).

Table 7
Calculated Gibbs free energy in kJ.

T (°C)	ΔG reaction (5)	ΔG reaction (6)	ΔG reaction (7)
0	−203.296	−39.455	−190.995
100	−228.428	−60.852	−166.146
200	−251.823	−81.482	−143.020
300	−273.634	−101.340	−121.458
400	−292.309	−119.612	−103.004
500	−311.861	−138.284	−83.648
600	−332.568	−157.488	−63.107
700	−352.748	−176.382	−43.070
800	−372.461	−194.994	−23.477
900	−391.755	−213.349	−4.285
1000	−410.669	−231.469	14.546

- Step 1

$$2NO_3^- + C = 2NO_2^- + CO_2(g) \quad (5)$$

$$NO_3^- + C = NO_2^- + CO(g) \quad (6)$$

- Step 2

$$NO_2^- + O_2 = NO_3^- \quad (7)$$

Reaction proposed for step 1 where the formation of nitrite and carbon oxides is thermodynamically feasible in the temperature range studied (Table 7). An experiment evidencing that soot combustion reaction occurs using oxygen of nitrate ion has been performed previously [18]. A $CuKNO_3ZrO_2$ catalyst extracted from the reactor after soot reaction at inert atmosphere shows FTIR energy absorption bands associated to the presence of nitrite ions (1268 cm^{-1}).

The reaction proposed for step 2 is also thermodynamically feasible (Table 5). To corroborate the feasibility of step 2, an experiment of potassium nitrite oxidation was carried out in air flow in thermogravimetric reactor. The nitrite oxidation with air of the gaseous phase occurs from 470 °C.

Aged catalysts practically maintain the same activity than fresh catalysts and this behavior is associated with the presence of remainder nitrate ions determined by the previously mentioned techniques.

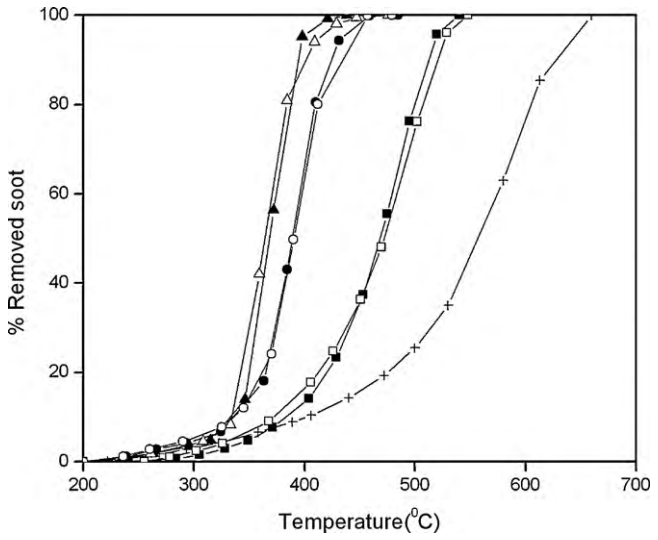

Fig. 6. Reactor of fixed bed. Fresh catalysts: (▲) KNO_3/Al_2O_3, (●) $Co/KNO_3/Al_2O_3$, and (■) Co/Al_2O_3. Aged catalysts: (△) KNO_3/Al_2O_3, (○) $Co/KNO_3/Al_2O_3$, and (□) Co/Al_2O_3. (×) Without catalyst.

4. Conclusions

Catalysts KNO_3/Al_2O_3 and $Co/KNO_3/Al_2O_3$ are the most active ones in the oxidation of soot. These fresh catalysts contain free nitrate ions in their composition while in the aged form they contain nitrate species interacted with the support.

The aging process of catalysts produces a significant change in catalyst redox properties. The reducibility of these catalysts with hydrogen is substantially lower than the one of fresh catalysts. The fresh $Co/KNO_3/Al_2O_3$ catalyst presents higher reducibility since several species contribute in the reduction process. Besides, it presents reducible species in the operation temperature range of the automobile exhaust pipe when it has been aged for 2 h at 800 °C.

In spite of this reducibility loss in hydrogen flow, all catalysts analyzed do not present a decrease of catalytic activity.

The stages of the reaction mechanism proposed, soot oxidation with oxygen from nitrate ion and subsequent oxidation of nitrite ion, are thermodynamically possible and there exist experimental data that support these facts.

Acknowledgements

Authors thank for the financial support of UNSL (Universidad Nacional de San Luis), UNLP (Universidad Nacional de La Plata), CONICET, Junta de Andalucía Proyecto de Excelencia P06-FQM-01661 and ANpCYT.

References

[1] S. Yuan, P. Mériaudeau, V. Perrichon, Appl. Catal. B 3 (1994) 319.
[2] J.P.A. Neeft, M. Makkee, J.A. Moulijn, Appl. Catal. B 8 (1996) 57.
[3] S. Wang, B. Haynes, Catal. Commun. 4 (2003) 591.
[4] A.L. Carrascull, C. Grzona, I.D. Lick, M.I. Ponzi, E.N. Ponzi, React. Kinet. Catal. Lett. 75 (2002) 63.
[5] J.A. Sullivan, O. Keane, L. Maguire, Catal. Commun. 6 (2005) 472.
[6] E. Cauda, D. Mescia, D. Fino, G. Saracco, V. Specchia, Ind. Eng. Chem. Res. 44 (2005) 9549.
[7] Y. Zhang, X. Zou, L. Sui, Catal. Commun. 7 (2006) 855.
[8] R. Jiménez, X. García, C. Cellier, P. Ruiz, A.L. Gordon, Appl. Catal. A 297 (2006) 125.
[9] Y. Zhang, X. Zou, Catal. Commun. 8 (2007) 760.
[10] J. Liu, Z. Zhao, C. Xu, A. Duan, L. Zhu, X. Wang, Appl. Catal. B 61 (2005) 36.
[11] H. An, P.J. McGinn, Appl. Catal. B 62 (2006) 46.
[12] I. Atribak, I. Such-Basáñez, A. Bueno-López, A. García, J. Catal. 250 (2007) 75.
[13] N.F. Galdeano, A.L. Carrascull, M.I. Ponzi, I.D. Lick, E.N. Ponzi, Thermochim. Acta 421 (2004) 117.
[14] B. Bialobok, J. Trawczynski, T. Rzadki, W. Mista, M. Zawadzki, Catal. Today 119 (2007) 278.
[15] X. Wu, D. Liu, K. Li, D. Weng, Catal. Commun. 8 (2007) 1274.
[16] Y. Zhang, Y. Qin, X. Zou, Catal. Commun. 8 (2007) 1675.
[17] S.A. Mosconi, I.D. Lick, A. Carrascull, M.I. Ponzi, E.N. Ponzi, Catal. Commun. 8 (2007) 1755.
[18] I.D. Lick, A. Carrascull, M.I. Ponzi, E.N. Ponzi, Ind. Eng. Chem. Res. 47 (2008) 3834.
[19] A.L. Carrascull, I.D. Lick, E.N. Ponzi, M.I. Ponzi, Catal. Commun. 4 (2003) 124.
[20] D. Hleis, M. Labaki, H. Laversin, D. Courcot, A. Aboukaïs, Colloid Surf. A: Physicochem. Eng. Aspects 330 (2008) 193.
[21] Y. Zhang, X. Zou, Catal. Commun. 7 (2006) 523.
[22] D. Bazin, I. Kovacs, L. Guczi, P. Parent, C. Laffon, F. De Groot, O. Ducreux, J. Lynch, J. Catal. 189 (2000) 456.
[23] A. Jones, B. Mc Nicol, Temperature Programmed Reduction for Solid Material Characterization, Marcel Dekker, Inc., NY, 1986, p. 104.
[24] P. Arnoldy, J.A. Moulijn, J. Catal. 93 (1985) 38.
[25] B. Ernst, L. Hilaire, A. Kiennemann, Catal. Today 50 (1999) 413.
[26] S. Hinchiranam, Y. Zhang, S. Nagamori, T. Vitidsant, N. Tsubaki, Fuel Process. Technol. 89 (2008) 485.
[27] L. Xue, C. Zhang, H. He, Y. Teraoka, Appl. Catal. B 75 (2007) 167.
[28] K. Nakamoto, Infrared and Raman Spectra of Inorganic and Coordination Compound, John Wiley and Sons, New York, 1992.
[29] T.J. Chuang, C.R. Brundle, D.W. Rice, Surf. Sci. 59 (1976) 413.
[30] A. Infantes-Molina, J. Mérida-Robles, E. Rodríguez-Castellón, J.L.G. Fierro, A. Jiménez-López, J. Catal. 240 (2006) 258.
[31] R. Moreno-Tost, E. Rodríguez-Castellón, A. Jiménez-López, J. Mol. Catal. A: Chem. 248 (2006) 126.
[32] A. Infantes-Molina, J. Mérida-Robles, E. Rodríguez-Castellón, B. Pawelec, J.L.G. Fierro, A. Jiménez-López, Appl. Catal. A 286 (2005) 239.
[33] K.S. Chung, F.E. Massoth, J. Catal. 64 (1980) 320.